Electronic Supplementary Material (ESI) for Materials Horizons.

Thermo-Growing Ion Clusters Enabled Healing Strengthening and Tough Adhesion for Highly Reliable Skin Electronics

Song Chen,[a,b] Xinyu Chen,[a] Kaiying Luo,[a] Wenwei Yang,[a] Xueling Yan, [a] Lan Liu* [a]

[a]School of Materials Science and Engineering, Key Lab of Guangdong Province for High Property and Functional Macromolecular Materials, South China University of Technology, Guangzhou, 510641, P. R. China

[b]School of Chemistry & Chemical Engineering, Anhui University, Hefei, Anhui, 230601, P. R. China

Contents

Supporting experimental section

Materials

Thioctic acid (TA, 99%), betaine (BT, 98%), and N,N,N',N'-tetrakis(2-hydroxyethyl) ethylenediamine (THEED, 99%) were purchased from Shanghai Macklin Inc. Ethanol was purchased from Tianjin Fuyu Fine Chemical Co., Ltd. All reagents were used as received without any post-treatment.

Preparation of polyTA-THEED$_\phi$-X elastomer

The TA monomer was totally dissolved in ethanol to obtain a TA solution firstly (0.5 g/mL, 500 rpm for 30 min). Then varying amounts of THEED were added into the TA solution and kept stirred for another 30 min to prepare the TA/THEED mixture solution. The obtained solution was poured into a Teflon mold and dried at ambient temperature for the total evaporation of ethanol solvent and the ROP of TA. After drying, the yellow transparent polyTA-THEED$_\phi$-0 solution based on weak ionic crosslinking was obtained. In this work, ϕ was adjusted from 10% to 40%. The polyTA-THEED$_\phi$-0 solution was stored in different elevated temperatures (vacuum oven heating at 70℃, 90℃, and 110℃, respectively) for the thermo-growth of ions to ion clusters. The gelation transition of solution to polyTA-THEED$_\phi$-X elastomer was obtained after heating X hours and cooling down to room temperature.

Preparation of BT composited polyTA-THEED$_\phi$-BT$_\lambda$-X ionic elastomer

The polyTA-THEED$_\phi$-BT$_\lambda$-X ionic elastomer was developed by introducing the zwitterionic BT into the polyTA-THEED$_\phi$-X elastomer. Specifically, the TA, THEED, and BT were gradually dissolved in ethanol to prepare mixture solution. During them, the BT molar ratio to TA, λ, was determined to 3%, 5%, 7%, 10%, and 15%, respectively. And the total mole amount of THEED and BT to TA was fixed to 35% (i.e. $\phi + \lambda = 35\%$). Then the mixture solution was also stored at ambient temperature for ethanol evaporation and at 70 ℃ for variable time to prepare solid ionic elastomer.

Structure characterization

Fourier transform infrared (FTIR) Fourier-transform infrared spectroscopy (FTIR) spectra were obtained using a German Bruker Vertex 70 Fourier transform infrared spectrometer, the transmission mode was applied. And the blank KBr sheet was used as the background for the sample coating and heating, the scan resolution was set to 4 cm^{-1}, 32 scans were performed to obtain the corresponding infrared spectra. The scanning range is 4000 cm^{-1}~500 cm^{-1}. Ultraviolet-visible

spectrophotometry (UV-vis) was performed using a UV755B ultraviolet-visible spectrophotometer (Shanghai Youke Instrument Co., Ltd., China) to test the TA-THEED/ethanol solution with different heating times and the anhydrous ethanol UV-visible absorption spectrum was used as the baseline. The concentration of TA-THEED/ethanol solution was diluted 400 times for UV-vis scanning, scanning resolution was set to 0.2 nm. Nuclear magnetic resonance spectroscopy (^{1}H-NMR) was tested using an AVANCE III HD 600 instrument (Bruker, Germany), and the sample dosage was 20-50 mg, which was dissolved in 0.6 mL deuterated DMSO. Transmission electron microscope (TEM) was carried out on a JEM-2100F electron microscope operating at 200 kV. A ~100 nm thin sectional sample was microtomed by a Leica EM FC7 microtome and collected on copper TEM grids from the top of water. Thermogravimetry (TG) was conducted on a TG 209 F1 instrument (NETZSCH-Gerätebau GmbH, Germany) to test the decomposition temperature of the samples.the nitrogen atmosphere, heating rate of 20 K/min, and temperature ranges from 30 ℃ to 700 ℃ were adopted. Differential scanning calorimetry (DSC) was tested to investigate the glass transition temperature of the samples using a DSC3500A-0208-L instrument (NETZSCH-Gerätebau GmbH, Germany). The test conditions were determined as nitrogen atmosphere, 10 K/min heating rate, and temperature ranges from -60 ℃ to 80 ℃. Rheology test was conducted on a torque rheometer (CFT-500D-PC, Tsushima, Japan) to measure the storage modulus (G') and loss modulus (G'') of the samples with dynamic frequency sweep (frequency sweep strain is 1%, shear strain rate The range is 0.1-100 rad/s) and constant-frequency variable-temperature scanning (the sweeping strain is 1%, the shear strain rate is 1 Hz, and the temperature is 20-120 ℃). The loss factor (tan δ) was calculated by G''/G'.

Molecular Dynamics (MD) Simulation

TA, THEED and ethanol were geometrically optimized by Gaussian 16[1] under SMD (ethanol) implicit solvation model with density functional theory B3LYP-D3(BJ)/def-TZVP level. Ambertools21[2] and ACPYPE[3] were used to construct the general AMBER force field 2(GAFF2) parameters[4], Multiwfn[5] was used to fit the restrained electrostatic potential 2(RESP2) charge[6]. MD simulations of TA-THEED systems with two different temperatures were performed using GROMACS 2021.5 package[7]. Intital cubic box with a size of 14×14×14 nm^3 was established by added 1040 TA (1 M), 520 THEED (0.5 M) and 13220 ethanol molecules. Energy minimization was performed using the steepest descent algorithm with a force tolerance of 1000 kJ mol^{-1} nm^{-1}. In

all the three directions, periodic boundary conditions were imposed. Then system was relaxed for 1 ns under NPT ensemble with different temperatures (298 K and 343 K) respectively and and cubic box size eventually stabilized at $12\times12\times12$ nm^3.

After completing the above steps, 300 ns NPT MD simulation was performed. Pressure was maintained at 1 bar by the Parrinello-Rahman barostat[8] in an isotropic manner and temperature was maintained at 298 K or 343 K by the V-rescal thermostat[9]. The LINCS algorithm was performed for constrain bond lengths of hydrogen atoms. Lennard-Jones interactions were calculated within a cutoff of 1.2 nm, and electrostatic interactions beyond 1.2 nm were treated with particle-mesh Ewald (PME) method with a grid spacing of 0.16 nm. All results were visualized by UCSF ChimeraX[10].

Mechanical and self-healing Test

Dumbbell samples with length of 35 mm were used for the fracture tensile stress test and tensile cycle tests at a testing speed of 0.4 /s. The tensile testing was applied using a tensile and compressive testing machine (KJ1065, Dongguan Kejian Testing Instrument Co., Ltd.).

For self-healing test, the dumbbell sample was cut into two pieces and then the fresh cut surfaces were put in contact. The two cut-off samples were then healed in different conditions for different periods. The healed samples were stretched following the same procedure to obtain the stress-strain curves. The mechanical healing efficiency was defined as the ratio between the restored fracture stress relative to the original fracture stress.

Self-adhesion Test

Three types of adhesive test were applied to character the tough adhesion of our elastomers: 90° peeling, lap-shear adhesion, and contact adhesion.

For 90° peeling test, the interfacial toughness was usually obtained by a 90° peeling test (ASTMD 2861) with a mechanical testing machine and a 90° peeling fixture. In the peeling test, polyethylene glycol terephthalate (PET), glass, aluminum (Al), iron (Fe), and polydimethylsiloxane rubber (PDMS) plates were used as the substrates. All the substrates were prepared with dimensions 7.6 cm in width, 12.7 cm in length and 0.3 cm in thickness. The PET films were used as stiff backing to support the samples. All tests were conducted in ambient air at room temperature. All the supramolecular elastomer samples were 110 mm × 30 mm × 6 mm in size. All the 90° peeling tests were performed with a constant peeling speed of 50 mm min^{-1}. The measured force reached a

plateau as the peeling process entered the steady state. The interfacial toughness Γ was determined by dividing the plateau force F by the width of the sample W. For self-adhesion toughening measurement, the supramolecular elastomer was attached onto different substrates, heated for a given time, and then cooled before test.

For the lap-shear adhesion measurement, two treated substrates are stacked together at ends by our elastomer (thickness: 2 mm). The width and length of the adhesion area are approximately 12.5 and 20 mm, respectively. The constant stretching rate is 20 mm/min. The lap shear strength is calculated by σ = F/S, where F is the maximum lap shear force and S is the area of the overlapping part. When pigskin is used as substrate, the fat under the porcine skins was removed with blade and the dermal surface of the porcine skin is cleaned with alcohol and gauze before the experiments.

For contact adhesion measurement, the bond area was a circle with a diameter of 8 mm and the sample thickness was about 2 mm. The test speed is 10 mm/min, the preload force is 100 gf, 500 gf and 1000 gf, respectively. The loading time is 30 s, and the substrate is aluminum. The bonding energy is calculated by the following formula:

$$W = \frac{\int F d_{\delta}}{A}$$

where F is Force, A is contact area, δ is displacement.

All the above-mentioned adhesion tests were carried out at room temperature using the tensile testing machine (KJ-1065A, Dongguan Kejian Instruments Co., Ltd. China)

Ionic conductivity test

The ionic conductivity was measured by TEGAM1740 digital micro-ohmmeter (TEGAM, America), the sample is 8 cm in length, 1 cm in width, and 2 mm in thickness.

Strain and wearable sensing performance test

The TEGAM1740 digital micro-ohmmeter (TEGAM, America) was used to measure and record the resistance changes under different strains, frequency cycles, and joint movements.

Skin impedance test

The skin contact impedance was recorded using an electrochemical workstation (CHI760E) and a dual electrode with an ionic elastomer as the interface between the copper sheet electrode and the skin of the arm. The distance between the adjacent edges of the two electrodes is 1.5 cm, and the test frequency range is $10^0 \sim 10^5$ Hz.

EMG signal test

The electromyographic sensor (Wuxi Sizhirui Technology Co., Ltd.) was used to measure and record the EMG signal. Two ionic elastic bodies are attached to the same arm muscle to be tested, and the other is attached to the stationary muscle for measurement. As a reference sample, the muscle electrical signals of the grip rings of different pounds and relaxation were collected.

ECG signal test

The ECG sensor (Heal Force PC80B, China) was used to measure and record the ECG signals. Three ionic elastic bodies are respectively attached to the upper right, upper left, and lower left positions of the chest and abdomen to collect the ECG signals at different times (0-24 h).

All the wearable sensing, skin impedance, EMG and ECG measurements were performed on human epidermal skin, there are no ethical concerns during the test, so the approval from a national or institutional ethics board/committee is not necessary. All the participants have provided written informed consent before the study was conducted.

Supporting Fig.s

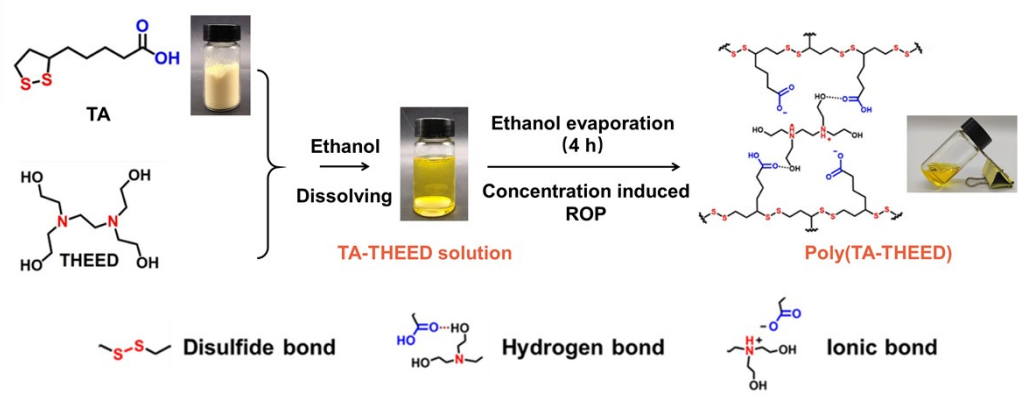

Fig. S1 Schematic illustration of the preparation of polyTA-THEED$_{\phi}$-0 solution. Insets are corresponding digital photos (in inset the ϕ = 35%).

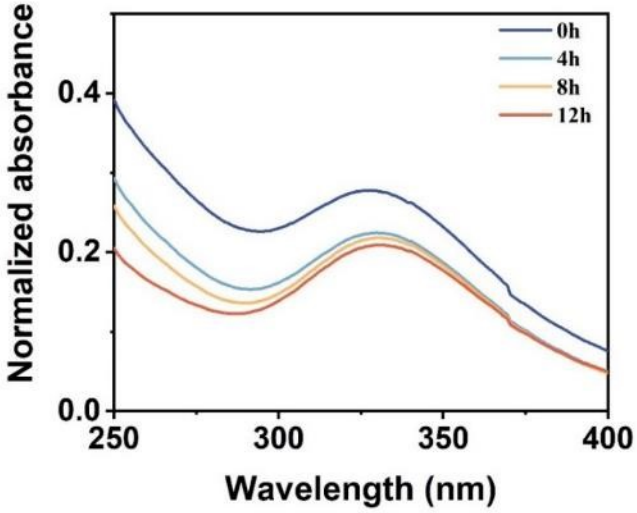

Fig. S2 UV-Vis spectrum of polyTA-THEED$_{0.35}$-0 solution with different storing time at room temperature.

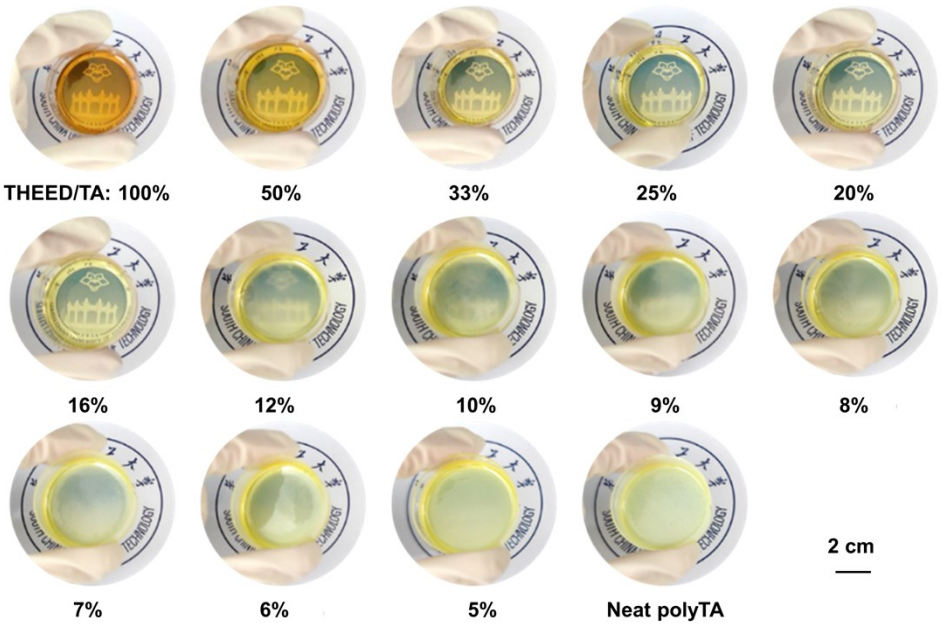

Fig. S3 Digital photographs of the polyTA and polyTA-THEED$_{\phi}$-0 with different amounts of THEED after storing at room temperature for 24 h without heating, showing the adding of THEED can prevent the depolymerization of polyTA.

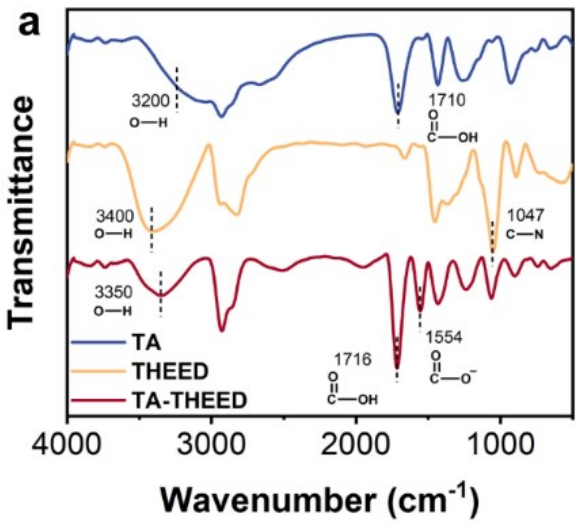

Fig. S4 FTIR spectra of TA, THEED, and polyTA-THEED$_{0.35}$-0

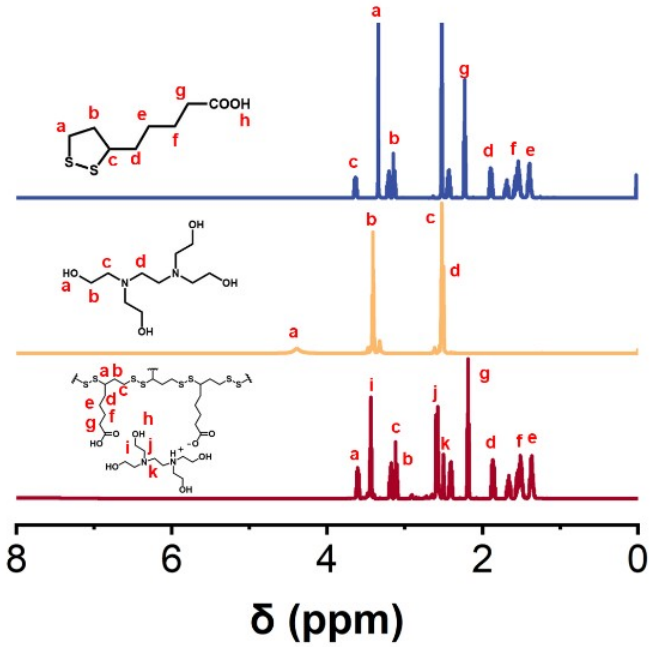

Fig. S5 ^{1}H NMR of TA, THEED and polyTA-THEED$_{0.35}$-0. The chemical shift and peak integrated area of each peak are as follows: For poly(TA-THEED)$_0$, ^{1}H NMR (600 MHz, DMSO): δ 3.60 (dq, J = 8.7, 6.2 Hz, 2H), 3.44 (d, J = 12.2 Hz, 1H), 3.18 (ddd, J = 10.9, 6.8, 5.5 Hz, 2H), 3.11 (dt, J = 10.9, 6.8 Hz, 2H), 2.59 (dd, J = 13.4, 7.2 Hz, 3H), 2.45 - 2.37 (m, 2H), 2.19 (t, J = 7.3 Hz, 4H), 1.86 (dq, J = 13.5, 6.8 Hz, 2H), 1.71 - 1.62 (m, 2H), 1.59 - 1.47 (m, 6H), 1.36 (dtdd, J = 10.3, 8.2, 6.2, 3.0 Hz, 4H). For THEED monomer, ^{1}H NMR (600 MHz, DMSO) δ 4.36 (s, 1H), 3.39 (t, J = 6.2 Hz, 12H), 2.51 (s, 3H), 2.48 (s, 3H). For TA monomer, ^{1}H NMR (600 MHz, DMSO) δ 11.99 (s, 1H), 3.61 (dq, J = 8.8, 6.2 Hz, 1H), 3.19 (ddd, J = 10.9, 6.9, 5.5 Hz, 1H), 3.11 (dt, J = 11.0, 6.8 Hz, 1H), 2.41 (dq, J = 12.5, 6.2 Hz, 1H), 2.21 (t, J = 7.3 Hz, 2H), 1.87 (dq, J = 13.5, 6.8 Hz, 1H), 1.71 - 1.62 (m, 1H), 1.59 - 1.49 (m, 3H), 1.51 - 1.46 (m, 1H), 1.37 (dddd, J = 16.5, 10.1, 7.2, 2.9 Hz, 2H).

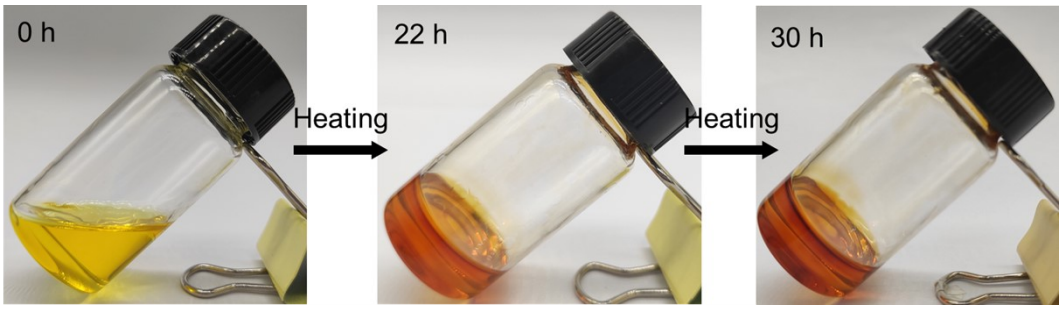

Fig. S6 Digital photographs of the polyTA-THEED$_{0.35}$-0 solution and elastomers after heating different time.

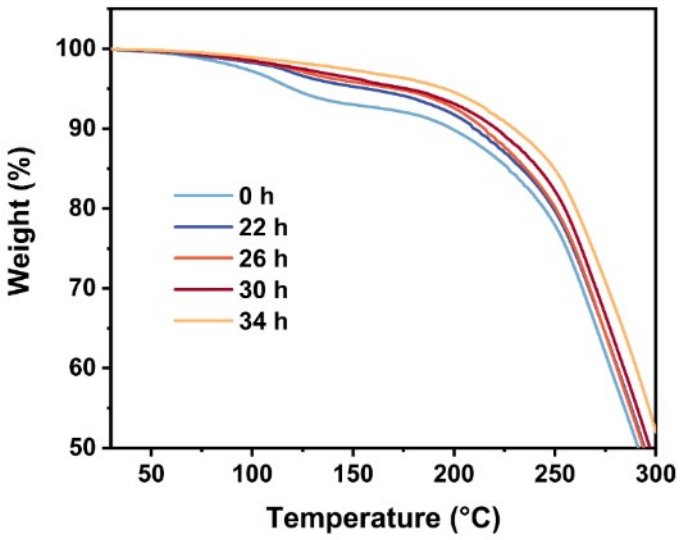

Fig. S7 Closeup TG curves of the polyTA-THEED$_{0.35}$-X with different heating time.

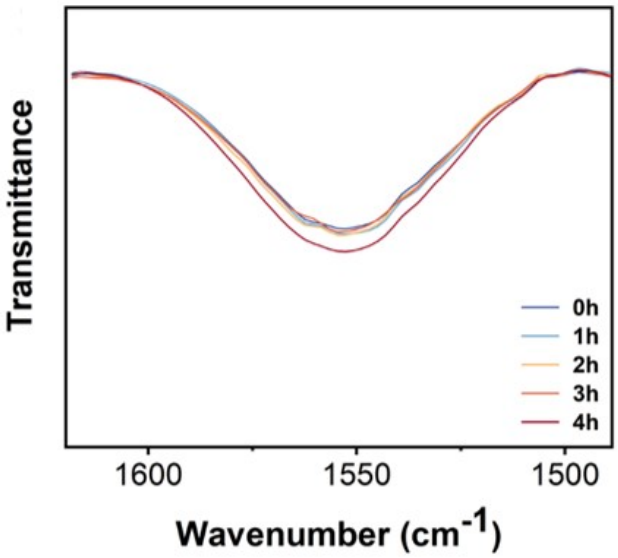

Fig. S8 Closeup FTIR curves of the polyTA-THEED$_{0.35}$-X with different heating time.

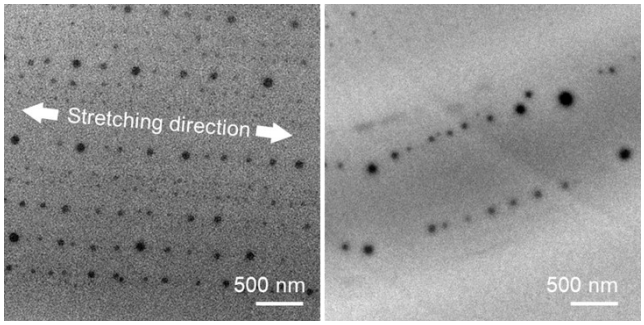

Fig. S9 TEM images of the polyTA-THEED$_{0.35}$-22 elastomer recovered from12000% strain

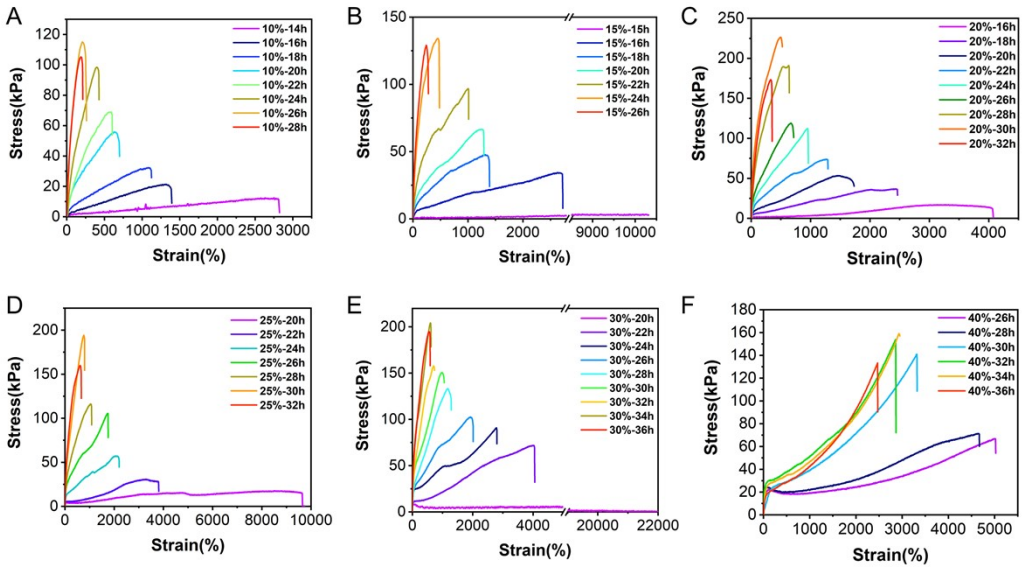

Fig. S10 Mechanical properties of polyTA-THEED$_{\phi}$-X elastomers with different THEED content and heating time. (Heating temperature: 70 °C. A: ϕ=10%; B: ϕ=15%; C: ϕ=20%; D: ϕ=25%; E: ϕ=30%; F: ϕ=40%).

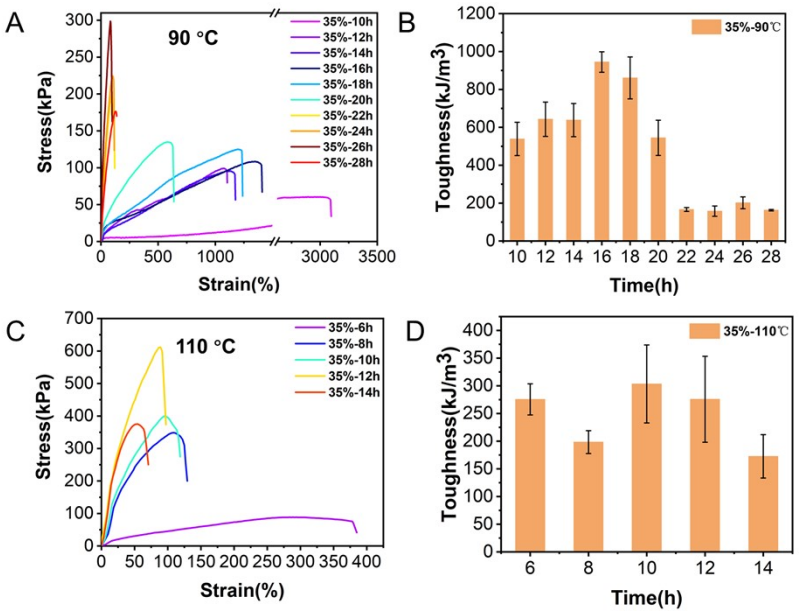

Fig. S11 Tensile properties and bulk toughness of polyTA-THEED$_{0.35}$-X elastomers heated at (A, B) 90 ℃ and (C, D) 110 ℃ for different time.

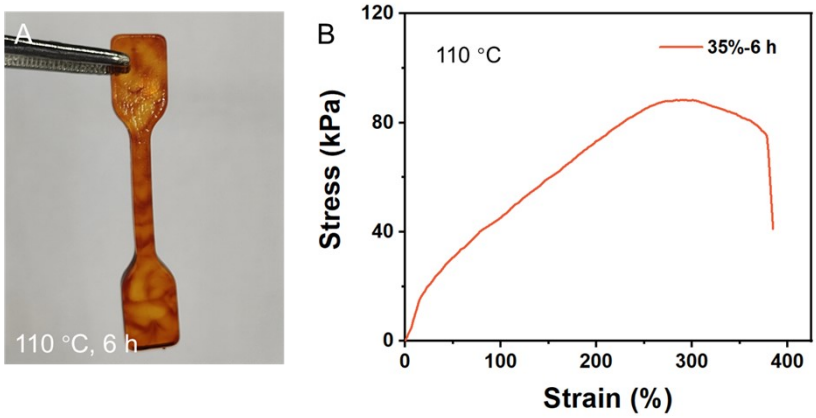

Fig. S12 Digital photo and stress-strain curve of polyTA-THEED$_{0.35}$-X elastomers heated at 110 ℃ for 6 h.

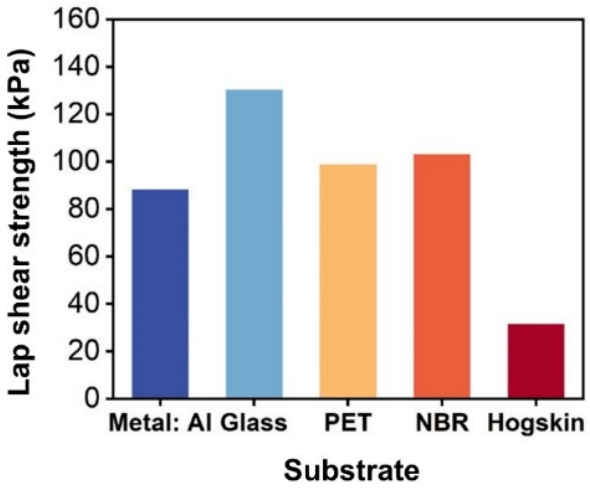

Fig. S13 Lap-shear strength of the polyTA-THEED$_{0.35}$-22 elastomer to different substrates.

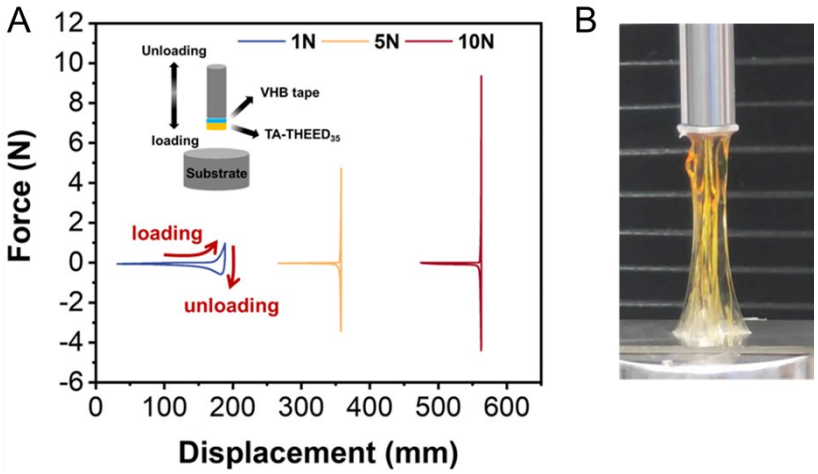

Fig. S14 A) Contact mechanics adhesion curves of the polyTA-THEED$_{0.35}$-22 elastomer, the insert is the schematic diagram of testing process. B) Digital photo of the polyTA-THEED$_{0.35}$-22 elastomer during unloading process.

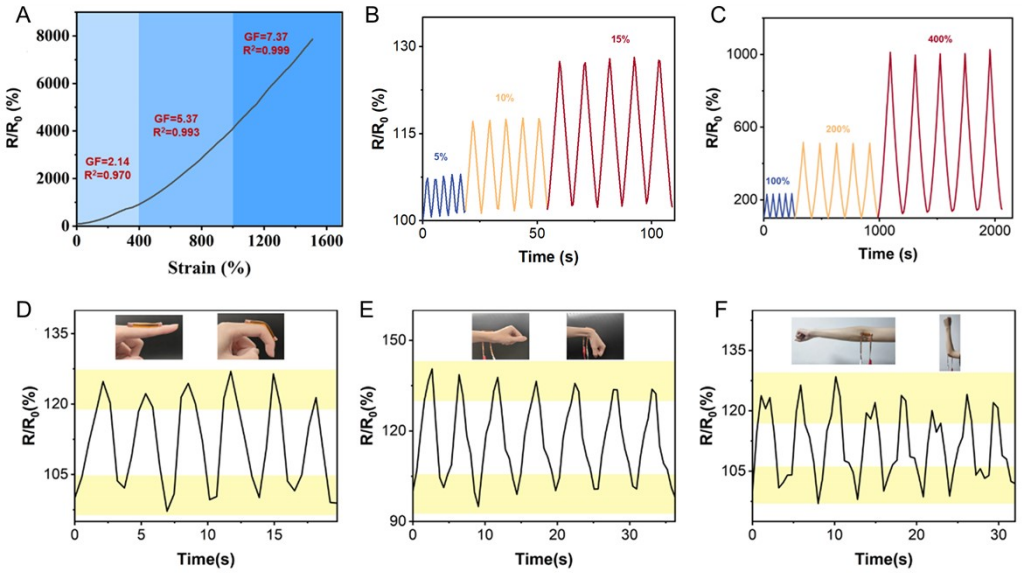

Fig. S15 A) The R/R_0 of the strain sensor as a function of strain and corresponding gauge factor (GF). B, C) Dynamic electric responses of the strain sensor under various strains. The related resistance changes of the polyTA-THEED$_{0.35}$-22 elastomer in response to (D) finger bending, (E) wrist bending, and (F) elbow bending.

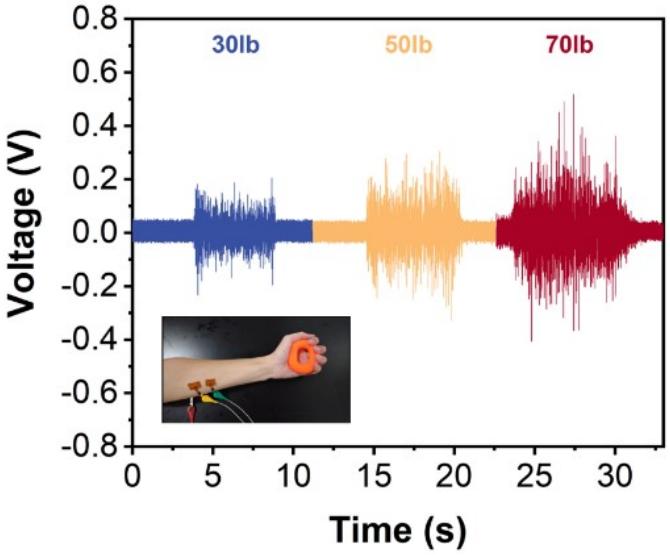

Fig. S16 EMG signals measured by the polyTA-THEED$_{0.35}$-22 elastomer as skin electrode (illustration shows the digital photo during testing).

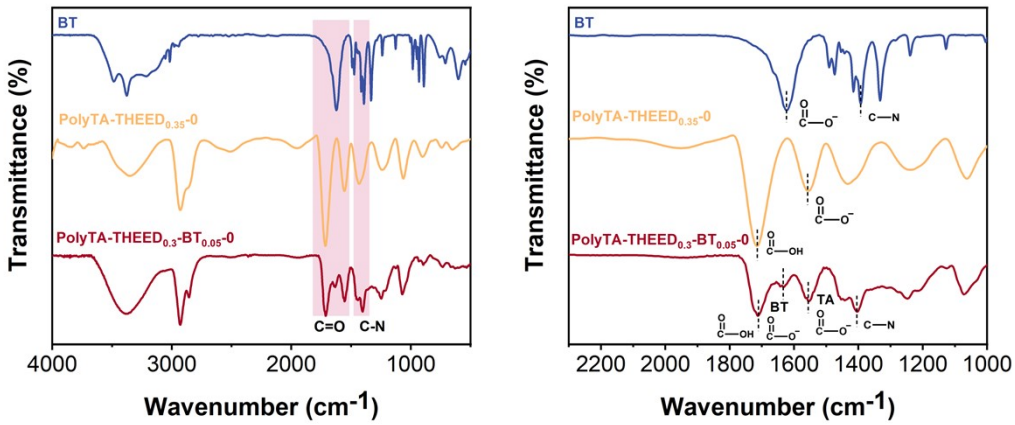

Fig. S17 FTIR spectrum of BT, polyTA-THEED$_{0.35}$-0, and polyTA-THEED$_{0.3}$-TB$_{0.05}$-0 ionic elastomers

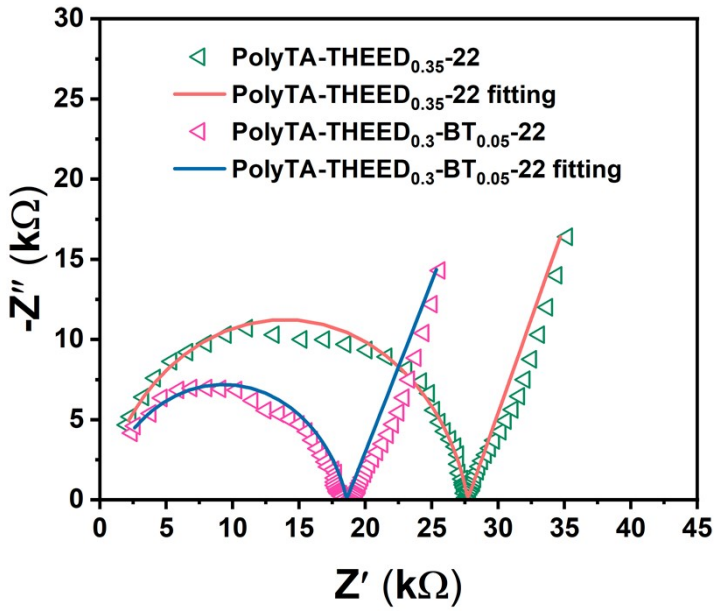

Fig. S18 The EIS curves of polyTA-THEED$_{0.35}$-22 and polyTA-THEED$_{0.3}$-TB$_{0.05}$-22 elastomers.

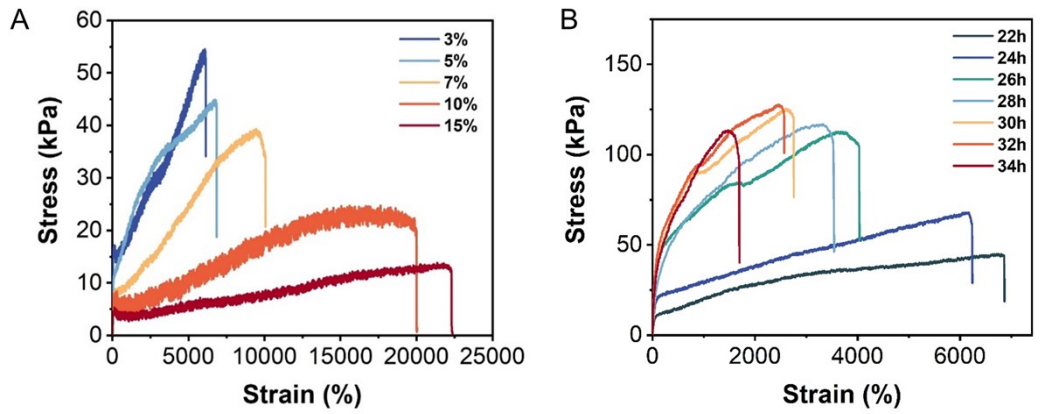

Fig. S19 A) The effect of BT content (A) and heating time (B) on the mechanical properties of the polyTA-THEED$_{\phi}$-TB$_{\lambda}$-22 ionic elastomers ($\phi + \lambda = 35\%$).

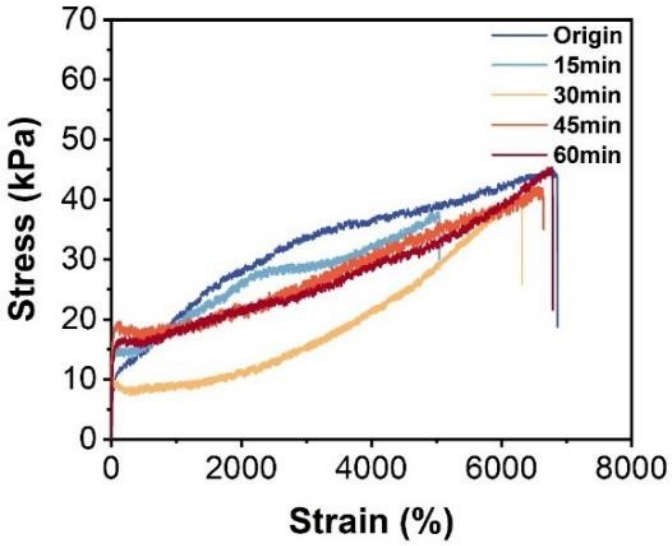

Fig. S20 Stress-strain curves of the polyTA-THEED$_{0.3}$-TB$_{0.05}$-22 ionic elastomers before and after self-healing at 25 ℃

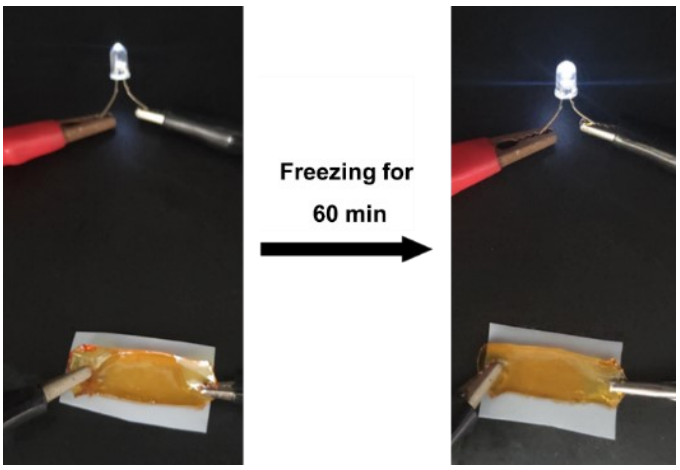

Fig. S21 Digital image of the polyTA-THEED$_{0.3}$-TB$_{0.05}$-22 ionic elastomer to illuminate a small light bulb before and after freezing at -20 ℃ for 60 min

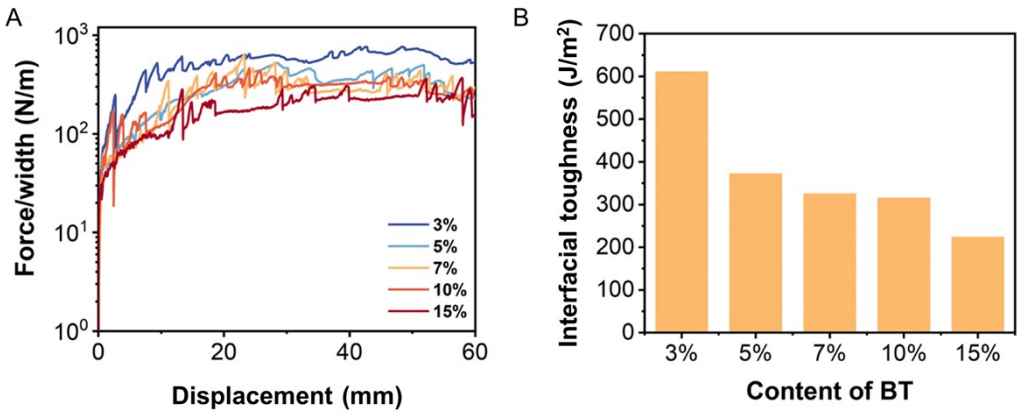

Fig. S22 Effect of BT content on the adhesion of the polyTA-THEED$_{\phi}$-TB$_{\lambda}$-22 ionic elastomers ($\phi + \lambda = 35\%$).

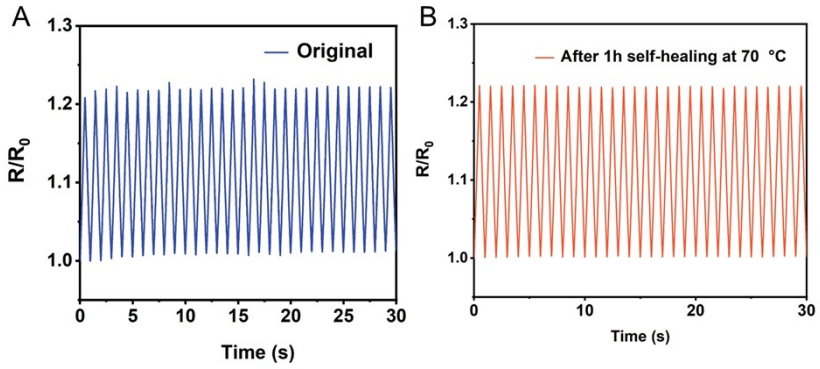

Fig. S23 Dynamic electric responses of the polyTA-THEED$_{0.3}$-TB$_{0.05}$-22 ionic elastomer to finger bending before (A) and after self-healing (B).

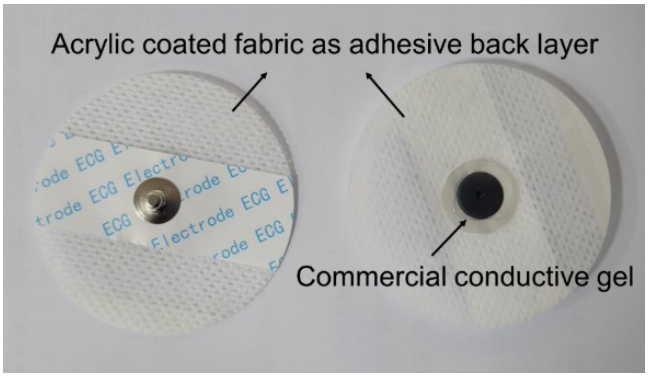

Fig. S24 Commercial ECG electrode with conductive hydrogel

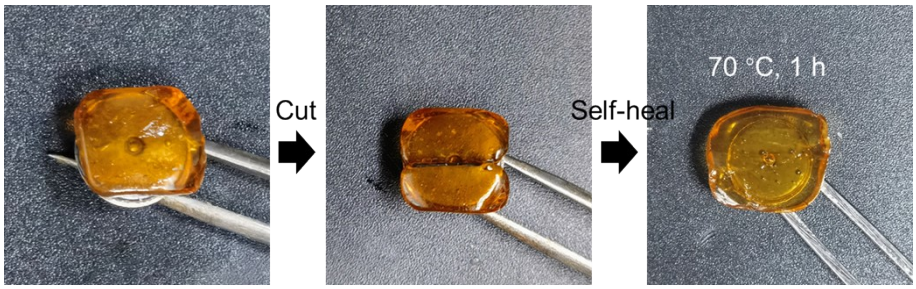

Fig. S25 Photographs of the skin-interfaced electrode for the EMG and ECG measurement before and after self-healing.

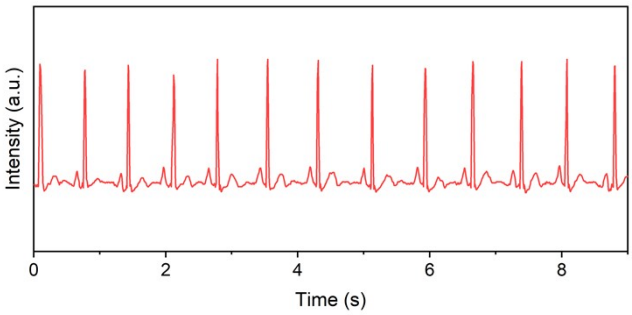

Fig. S26 EMG signals measured by polyTA-THEED$_{0.3}$-TB$_{0.05}$-22 ionic elastomer after 1 h self-healing at 70 °C.

Supporting Table

Table S1 Thermodynamic properties of polyTA-THEED$_{0.35}$-X elastomer

Heating time (h)	Tg (℃)	$T_{d5\%}$ (℃)	Residual mass fraction (%)
22	-36.3	156.9	3.42
26	-32.1	170.0	4.19
30	-28.2	176.7	3.31
34	-25.3	194.9	3.79

Supporting References

[1] Gaussian 16, Revision A.03, M. J. Frisch, G. W. Trucks, H. B. Schlegel, G. E. Scuseria, M. A. Robb, J. R. Cheeseman, G. Scalmani, V. Barone, G. A. Petersson, H. Nakatsuji, X. Li, M. Caricato, A. V. Marenich, J. Bloino, B. G. Janesko, R. Gomperts, B. Mennucci, H. P. Hratchian, J. V. Ortiz, A. F. Izmaylov, J. L. Sonnenberg, D. Williams-Young, F. Ding, F. Lipparini, F. Egidi, J. Goings, B. Peng, A. Petrone, T. Henderson, D. Ranasinghe, V. G. Zakrzewski, J. Gao, N. Rega, G. Zheng, W. Liang, M. Hada, M. Ehara, K. Toyota, R. Fukuda, J. Hasegawa, M. Ishida, T. Nakajima, Y. Honda, O. Kitao, H. Nakai, T. Vreven, K. Throssell, J. A. Montgomery, Jr., J. E. Peralta, F. Ogliaro, M. J. Bearpark, J. J. Heyd, E. N. Brothers, K. N. Kudin, V. N. Staroverov, T. A. Keith, R. Kobayashi, J. Normand, K. Raghavachari, A. P. Rendell, J. C. Burant, S. S. Iyengar, J. Tomasi, M. Cossi, J. M. Millam, M. Klene, C. Adamo, R. Cammi, J. W. Ochterski, R. L. Martin, K. Morokuma, O. Farkas, J. B. Foresman, and D. J. Fox, Gaussian, Inc., Wallingford CT, 2016.

[2] Case D A, Aktulga H M, Belfon K, et al. Amber 2021[M]. University of California, San Francisco, 2021.

[3] Wang J, Wang W, Kollman P A, et al. Automatic atom type and bond type perception in molecular mechanical calculations[J]. Journal of molecular graphics and modelling, 2006, 25(2): 247-260.

[4] Wang J, Wolf R M, Caldwell J W, et al. Development and testing of a general amber force field[J]. Journal of computational chemistry, 2004, 25(9): 1157-1174.

[5] Lu T, Chen F. Multiwfn: a multifunctional wavefunction analyzer[J]. Journal of computational chemistry, 2012, 33(5): 580-592.

[6] Schauperl M, Nerenberg P S, Jang H, et al. Non-bonded force field model with advanced restrained electrostatic potential charges (RESP2)[J]. Communications chemistry, 2020, 3(1): 1-11.

[7] Abraham M J, Murtola T, Schulz R, et al. GROMACS: High performance molecular simulations through multi-level parallelism from laptops to supercomputers[J]. SoftwareX, 2015, 1: 19-25.

[8] Pettersen E F, Goddard T D, Huang C C, et al. UCSF ChimeraX: Structure visualization for researchers, educators, and developers[J]. Protein Science, 2021, 30(1): 70-82.

[9] Nosé S, Klein M L. Constant pressure molecular dynamics for molecular systems[J]. Molecular Physics, 1983, 50(5): 1055-1076.

[10] Bussi G, Donadio D, Parrinello M. Canonical sampling through velocity rescaling[J]. The Journal of chemical physics, 2007, 126(1): 014101.